

باشر الطل الهندسى للحمو على عمليه تبريد الهواء
التبخري والترطيب فى غرفه رش ذات سريان عرضي

THE INFLUENCE OF PACKING GEOMETRY
ON THE EVAPORATIVE AIR COOLING AND
HUMIDIFICATION PROCESS IN A CROSS FLOW SPRAY CHAMBER

Barakat H. Z.* Sayed Ahmed E. S.** Oweis A. E.***

* Prof. Faculty of Engineering Ain Shams Univ.

** Ass. Prof. Faculty of Engineering Zagazig Univ.

*** Assistant Lecturer Faculty of Eng., Zagazig Univ.

خلاصه: اجريت تجارب على نوعين من الحشو لهما نفس مساحه
المقطع. احدهما مستو والاخر معرج لدراسة تاثير الحشو و
خواصه الهندسيه على عملية تبريد الهواء التبخري. وقد وجد
ان استخدام الحشو دى السطح المعرج افضل من دى السطح
المستو وذلك بالنسبه لعملية انتقال الحرارة والكتله خصوصا
عند اصغر نسب من الماء الى الهواء.
تم النوصل الى علاقات تجريبية تربط المعاملات لانتقال
الحرارة والكتله.

ABSTRACT :

The influence of packing and its geometry on the evaporative air cooling and humification processes are investigated in this study, where the experimental tests are carried out on two mats, flat and corrugated, having the same surface area. It was found that the corrugated packing enhances the heat and mass transfer processes better than the fiat mat, specially at the smallest water to air flow rate ratios (L/G).

Empirical relations for the variation of the heat and mass transfer available coefficients, $\left[\frac{h_M A_H}{G C_{pm}} \right]$ and $\left[\frac{h_M A_M \rho_a}{G} \right]$, with (L/G) and air Reynolds number (Re) are given.

NUMENCLATURE :

A_H, A_M = Heat and Mass transfer areas, respectively, m^2 .

C_{pm} = Specific heat of moist air at constant pressure, $KJ/Kg\ ^\circ C$

G = Air flow rate, $Kg/hr.$

h_H = Heat transfer coefficient, $KJ/m^2\ hr\ ^\circ C$

h = Mass transfer coefficient, $m/hr.$

L = Recirculated water flow rate, $kg/hr.$

l = test section length, m

$R_e = \frac{\rho_a V_a l}{\mu}$
Reynolds number.

$T_{db_{in}}, T_{db_{out}}$ = Dry bulb temperature of air just upstream and downstream of the test section, respectively, $^\circ C$

$T_{vb_{in}}, T_{vb_{out}}$ = Wet bulb temperature of air just upstream and downstream of the test section, respectively, $^\circ C$.

V_a = Bulk air mean velocity, $m/s.$

ρ_a = Bulk air mean density, Kg/m^3

$$\eta_H = \frac{W_{out} - W_{in}}{W_i - W_{in}} \times 100$$

W_{in}, W_{out} = Humidity ratio of air just upstream and downstream of the test section kg_v/kg_a

W_i = Humidity ratio of saturated air at the interface kg_v/kg_a

INTRODUCTION :

The needs for indoor humidifications continue to grow. Commercial buildings contain equipment such as copiers, computers, printers and other office machines that do not function well with in dry air, thereby stimulating the need

for humidification. New products, many of which require a humidified atmosphere during production, add to the need in industrial plants.

Gas turbine output can be increased, during periods of high ambient temperature, by using conditioned inlet air [1].

One of the most common processes in the industrial plant is the dissipation of heat and probably the most common way to dissipate heat is with an evaporative cooling tower. A cooling tower can be a cost effective way to cool vacuum deposition equipment [2]. Bantz and John A. [3] discussed a method for predicting and improving cooling tower performance.

The simultaneous heat and mass exchange takes place in evaporative cooling equipment due to the contact of air with water [4]. The efficiency of heat/mass exchange depends on the state of water and air, as well as, on surface or volume of evaporation. The calculation of equipment performance is complicated due to the simultaneous heat and mass transfer processes, since it is difficult to get a direct analytical solution of heat and mass transfer especially for turbulent flow. Therefore, experimental approaches are recommended.

An experimental investigation on the performance of water spray cross flow humidifier through the continuous circulation of water was previously discussed by Barakat H, Z. et al [5]. They presented the heat transfer results, through spray chamber, in dimensionless form in which

$\left[\frac{h_H A_H}{G C_{pm}} \right]$ was presented as a function of (Re) and (L/G) .

From this relationship, it was found that $\left[\frac{h_H A_H}{G C_{pm}} \right]$ is proportional to (Re) , to the power 0.23 and (L/G) to the

power 1.296. Also the evaporation results were presented in dimensionless form in terms of $\left[\frac{h_m A_m \rho_a}{G} \right]$ which was given as a function of (Re) and (L/G). From this relationship, it was found that $\left[\frac{h_m A_m \rho_a}{G} \right]$ is proportional to (Re) to the power 0.14 and (L/G) to the power 1.296.

The performance of wetted media type evaporative coolers under various conditions of operation, various design parameters was investigated on various types of packings [6,7]. For the same spray chamber size the use of packing media enhances the air washer performance. For the same packing material and surface area the packing geometry would have some influence on the evaporative air cooling equipment. For this reason, the effect of the packing geometry on the performance of the air washer is investigated in this work. For this purpose an experimental study have been carried out on cross flow spray chamber using flat and corrugated galvanized steel mesh with the same surface area, as it will be discussed below.

2. Experimental apparatus and packing :

2.1 Experimental apparatus :

The apparatus used in this study, Fig. (1), consists of a galvanized steel rectangular tunnel. The tunnel is divided into two portions, the first of which has (30 x 30 cm) cross sectional area and contains a cross flow spray washer. An electrical air pre-heater of variable capacity is installed in the tunnel inlet. The spray washer and the pre-heater are installed to control the air condition before entering to the test section. The second portion represents the test section and has (40 x 40 cm) cross-sectional area and is a cross flow spray chamber. The test section consists

of a casing containing a spray bank of 4 tubes each of which has 33 holes of 1 mm diameter, a tank for the collection of sprayed water and an eliminator section at the discharge end for the removal of entrained droplets of water from air. A pump recirculates water from the collector tank to the spray bank through a piping system.

The air flow is measured by a calibrated sharp-edged orifice meter and the rate of air flow is controlled by a sliding door as shown in Fig. (1). Calibrated copper-constantan thermocouples are used for temperature measurements. The air temperature at the inlet and outlet of the test section is measured, by 32 thermocouples which are fixed on two screens, one of which is installed upstream of the test section and the other downstream.

The cross section of the duct (40 x 40 cm) is divided into 18 equal rectangular areas and a thermocouple junction is placed at the center of each rectangle. Also, 18 thermocouples are fixed and equally distributed, on two screens with cross sectional area of (30 x 30 cm), installed up and down-stream.

The wet bulb temperature of air stream is measured by calibrated wetted-wick thermometers, which are inserted into the duct perpendicular to the air flow just up and downstream of both the test section and spray washer.

The flow rate of recirculated water flow is measured by a calibrated sharp-edged orifice. The water flow rate is controlled by a gate valve on the delivery side. The water temperature at inlet to the spray bank and at the water surface in the collecting pan are measured by two thermocouples, [7]. Metallic packing is placed in the test section and it is sprayed with recirculating water issuing from the tube bank.

2.2 Packing :

Two mats of packing are used in this study, where the two mats have the same surface area but are different in the geometrical shape. The packing material is galvanized steel mesh. The first mat is made of four interfering flat mesh boxes whose dimensions are shown in Fig. (2). The second mat is made of four layer corrugated mesh, whose dimensions are shown in Fig. (3). The air flow is parallel to the longitudinal axis of the packing while the water spray is perpendicular to them.

In the following paragraphs the performance of the air washer using the two types of packings is discussed and compared to its characteristics without the packing and the effect of the packing geometry is examined.

3. Results and discussion :

3.1 Humidification system performance during the nonadiabatic behavior in presence of the flat mat of packing

The results presented in [5] show that some deviation from the adiabatic humidification behavior takes place during humidification by water spraying, this section shows the humidifier characteristics when using the flat mat of packing during the nonadiabatic humidification behavior.

It worth mentioning here that where water is considered as the system, then pump work and associated energy losses which is added to the circulating water cause deviation from conditions established for adiabatic saturation process [5].

The experimental results plotted in Fig. (4) show the variation of humidifying efficiency (η_H) with water flow rate (L) at different air velocities (V_a). This graph shows that at constant air velocity (V_a), the humidifying efficiency (η_H) increases as the water flow rate (L)

increases. Also, it can be seen that the increase in air velocity (V_a) leads to decrease in efficiency (η_H). The maximum efficiency (η_H) is 75 % and it is obtained at the lower air velocity 1 m/s.

As expected, the humidification in presence of flat packing increases the humidifying efficiency (η_H) than the humidification without packing. Where it can be noted that the max. efficiency (η_H) increased from 63.5 % without the packing as reported in [5] to 75 % in this case due to the flat mat influence.

Figures 5 and 6 shows the variation of each $\left[\frac{h_H A_H}{G C_{pm}} \right]$ and $\left[\frac{h_M A_M \rho_a}{G} \right]$ with water to air ratio (L/G) at different air velocities (V_a) for the flat mat packing. It can be seen from these graphs that the increase of both $\left[\frac{h_H A_H}{G C_{pm}} \right]$ and $\left[\frac{h_M A_M \rho_a}{G} \right]$ with (L/G) is a linear. The relationship between these parameters are represented by:

$$\left[\frac{h_H A_H}{G C_{pm}} \right] = 0.0045 (L/G)^{0.95} (Re)^{0.434} \quad (1)$$

$$\left[\frac{h_M A_M \rho_a}{G} \right] = 0.0381 (L/G)^{0.95} (Re)^{0.245} \quad (2)$$

These equations represent the humidification system behavior through the nonadiabatic condition in presence of flat surface packing. The graphical displays of these equations are presented in Figs. (7) and (8) where $\left\{ \left[\frac{h_H A_H}{G C_{pm}} \right] / (Re)^{0.434} \right\}$ and $\left\{ \left[\frac{h_M A_M \rho_a}{G} \right] / (Re)^{0.245} \right\}$ are plotted versus (L/G). It is seen from these figures that all the data are contained within about ± 6 % band around the correlating lines.

Through examination of the graphs of Figs. (4 to 8), it can be observed that the heat and mass transfer available coefficients $\left[\frac{h_M A_H}{G C_{pm}} \right]$ and $\left[\frac{h_M A_M \rho_a}{G} \right]$ increased, in presence of flat mat by 18 % and 22.5 % respectively at $L/G = 2$ and by 38 % and 42 % at $L/G = 12$ as compared with the humidification without packing reported in [5] at $Re = 5.4 \times 10^4$. For $Re = 8.7 \times 10^4$, the values of $\left[\frac{h_H A_H}{G C_{pm}} \right]$ and $\left[\frac{h_M A_M \rho_a}{G} \right]$ increased by 40 % and 60 % at $L/G = 1.3$ and by 70 % and 80 % at $L/G = 0.78$.

From these results, it can be found that the flat surface packing has a noticeable effect on the heat and mass transfer processes specially at low water to air ratios ($L/G = 0.78 - 1.3$).

3.2 Humidification system performance during the nonadiabatic behavior in presence of corrugated mat packing :

The graphs of Figs. (9 to 11) show the experimental relationship of the available coefficients $\left[\frac{h_H A_H}{G C_{pm}} \right]$ and $\left[\frac{h_M A_M \rho_a}{G} \right]$ with water to air ratio (L/G) at different air velocities (V_a) on the log-log coordinates. From these graphs, it is seen that at constant air velocity (V_a) the available coefficients $\left[\frac{h_H A_H}{G C_{pm}} \right]$ and $\left[\frac{h_M A_M \rho_a}{G} \right]$ vary linearly with the water to air ratio (L/G) on log-log coordinates as the same for humidification with flat surface mat. However, the corrugation increases each of $\left[\frac{h_H A_H}{G C_{pm}} \right]$

and $\left[\frac{h_M A_M \rho_a}{G} \right]$ by 35 % and 42 % respectively compared with flat surface packing results for the same air velocity ($V = 1 \text{ m/s}$) and approximately the same inlet air condition.

The humidifier behavior with corrugated surface packing through the nonadiabatic condition is represented by the following power-law equations :

$$\left[\frac{h_H A_H}{G C_{pm}} \right] = 0.0185 (L/G)^{0.785} (Re)^{0.320} \quad (1)$$

$$\left[\frac{h_M A_M \rho_a}{G} \right] = 0.07 (L/G)^{0.785} (Re)^{0.40} \quad (2)$$

The graphical representation of these correlations are presented in Figs. (12 and 13) where $\left\{ \left[\frac{h_H A_H}{G C_{pm}} \right] / (Re)^{0.320} \right\}$

and $\left\{ \left[\frac{h_M A_M \rho_a}{G} \right] / (Re)^{0.40} \right\}$ are plotted versus (L/G) . It is seen from these figures that the data are contained within a $\pm 9 \%$ in Fig. (12) and a $\pm 7 \%$ in Fig. (13) around the correlating line.

3.3 Influence of the Packing Geometry on Humidifying Efficiency :

The object of this section is to further investigate the effect of the packing geometry on air humidification process during nonadiabatic recirculation of water. Fig.(14) shows the change in humidifying efficiency (η_H), for the two mats of packing, with water flow rate (L). It can be noted from the figure that at the same air velocity (V_a) and constant inlet air condition, the corrugated mat gives an increase in efficiency (η_H) about 26 % than the flat surface mat. Also the available coefficients of heat and mass transfer multiplied with the transferring area are increased by 40 % and 45 % respectively due to corrugation effect as shown in graphs of Figs. (15 and 16).

From the previous discussion, it can be noted that better results are given by the corrugated mat packing. This means that for the same packing area the packing geometry is an important parameter in the humidification process.

CONCLUSION :

The performance of water spray cross flow humidifier has been experimentally investigated during the continuous recirculation of water in presence of flat and corrugated mat packings with the same area. The influence of packing geometry on air humidification process was investigated. The following conclusions can be stated :

- * The packing enhances the heat and mass transfer processes specially at the smallest water to air ratios(L/G). However, at an air velocity of 1 (m/s) the increase of heat and mass available coefficients

$$\left[\frac{h_H A_H}{G C_{pm}} \right] \text{ and } \left[\frac{h_M A_M \rho_a}{G} \right] \text{ due to the flat mat influence are 16 \% and 22.5 \% respectively at } L/G = 2,$$

$$\text{while at } L/G = 1.2 \text{ the increase of } \left[\frac{h_H A_H}{G C_{pm}} \right] \text{ and}$$

$$\left[\frac{h_M A_M \rho_a}{G} \right] \text{ are 38 \% and 42 \% respectively.}$$

- * The shape of the packing has a considerable influence on the heat and mass transfer processes in the humidification process by water spraying. The corrugated mat packing gives a better humidifying efficiency than the flat mat of packing for the same surface area and inlet air condition. It also showed more improvement in

$$\text{heat and mass transfer available coefficients } \left[\frac{h_H A_H}{G C_{pm}} \right]$$

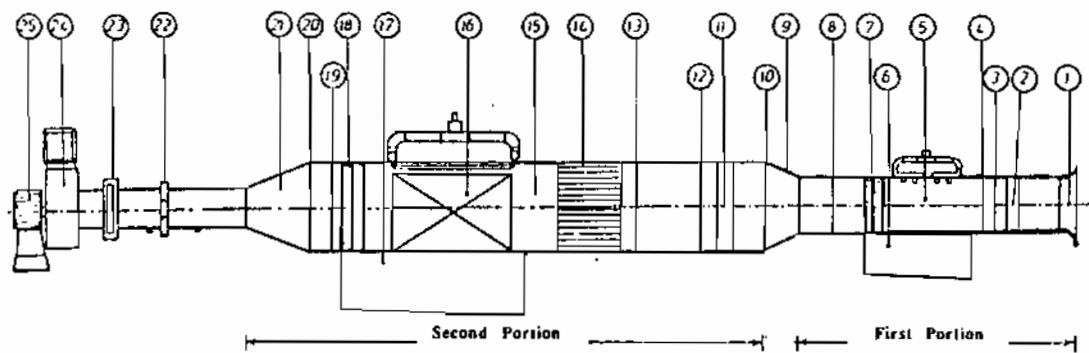
$$\text{and } \left[\frac{h_M A_M \rho_a}{G} \right] \text{ which were increased by 40 \% and 45 \% respectively as compared with the flat mat results.}$$

- * The variation of both of $\left[\frac{h_M A_M}{G C_{pm}} \right]$ and $\left[\frac{h_M A_M \rho_a}{G} \right]$ with Re follows in general a logarithmic relationship as given by the equations 1 through 4.

REFERENCES :

1. Sengupta, Utpal; Soroka, Gregory "Inlet air washer/chiller system for combined cycle plant repowering" proceedings of the 5th American power conference of Illinois/Inst of Technology USA. Apr 1989, Vol. 51, PP 248-252.0
2. Zahniser, David J. "Practical consideration in the design and operation of cooling towers for use with vacuum process equipment" Proceeding of the 33rd Annual Technological conference, New Orleans, LA, USA May 1990 PP 284-286.
3. Bartz, John A. "Predicting and improving cooling Tower performance" Power Engineering J. V. 94. n3 mar 1990 PP 35 - 37.
4. L. D. Berman, "Evaporative cooling of circulating water", Pergamon press London, 1961.
5. H. Z. Barakat, Sayed Ahmed E. S. Owais E. E. "On the simultaneous Heat and Mass transfer in a cross flow spray chambers" Ain Shams University, Engineering Bulletin Vol. 27, No. 1, Mars 1992. PP 322-340.
6. M. I. M. Nega, "Effectiveness of Wetted Media Evaporative Air Coolers Made from Natural Fibers" The Sixth Sympos., Sept. 1988, Menoufia University.

7. Y. Yu Liu and H. E. Hesketh, "Simultaneous Heat and Mass Transfer in Gaternary Cooling Tower " J. Engineering for Gass Turbines and Power, July, 1987, Vol. 109. PP. 245 - 248.



- | | | | | | |
|------------------------|------------------------|-----------------------|-------------------------|-------------------------|------------------------|
| 1- Entrance Section | 5- Air Washer | 9- Diffuser | 13- Thermocouple Screen | 17- Collector Tank | 21- Transition Section |
| 2- Electrical Heater | 6- Collector Tank | 10- Screen | 14- Tube Bundle | 18- Eliminator | 22- Orifice Meter |
| 3- Screen | 7- Eliminator | 11- Electrical Heater | 15- Test Section | 19- Screen | 23- Sliding Door |
| 4- Thermocouple Screen | 8- Thermocouple Screen | 12- Screen | 16- Packing | 20- Thermocouple Screen | 24- Centrifugal Fan |
| | | | | | 25- Fan Motor |

Fig. (1.) Sectional View of Apparatus.

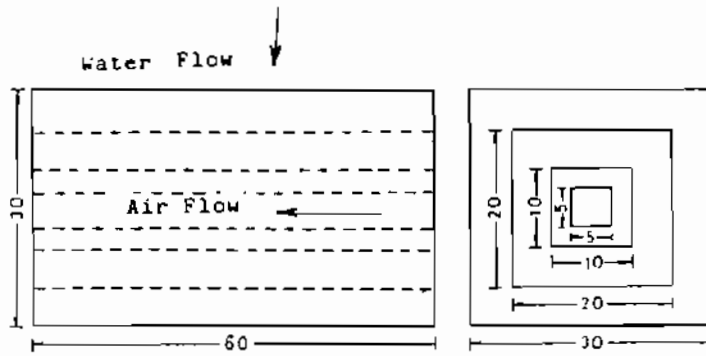


Fig. (2) Flat Mat Packing.

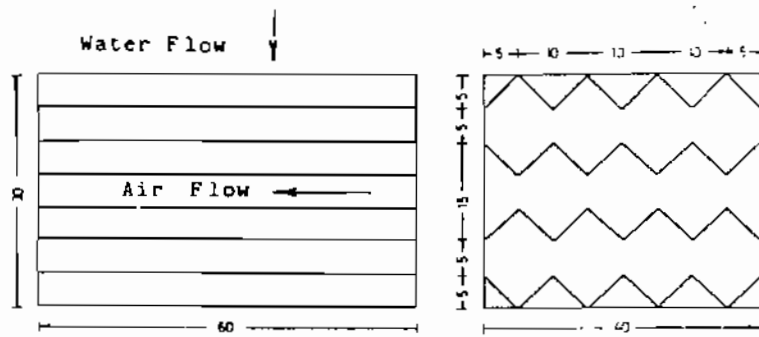


Fig. (3) Corrugated Mat Packing.

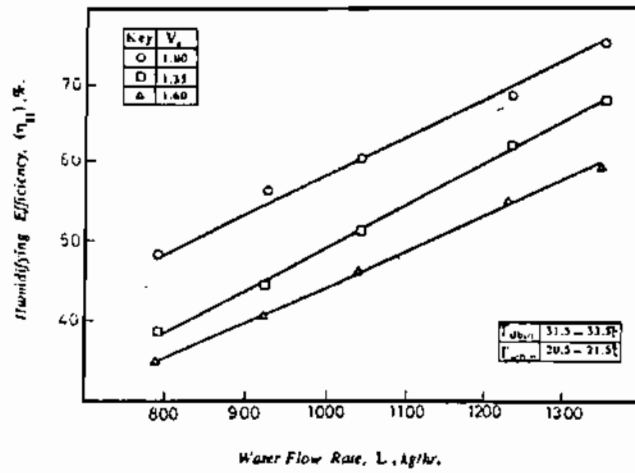


Fig (4) Variation of Humidifying Efficiency (η_{II}) with Water Flow Rate (L). for Flat Mat.

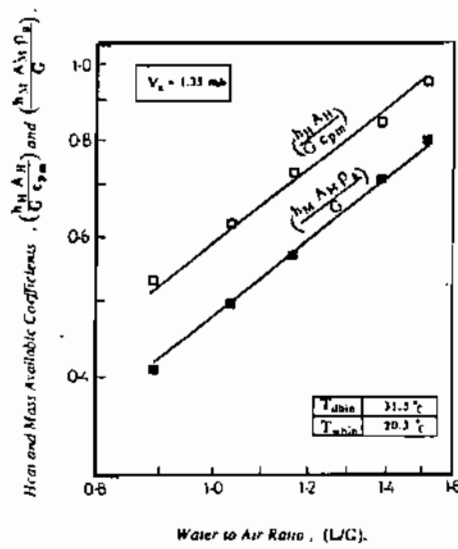


Fig (5) Variation of $\left(\frac{h_{II} A_{II}}{G c_{pm}}\right)$ and $\left(\frac{h_{M} A_{M} P_A}{G}\right)$ with (L/G) for $Re = 7.39 \cdot 10^4$ for Flat Mat.

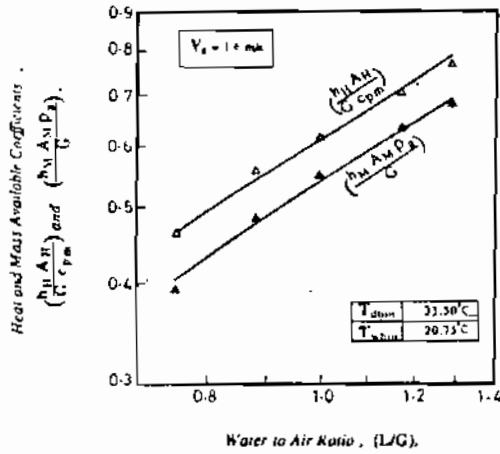


Fig. (6) Variation of $(\frac{h_M A_M}{G c_{pM}})$ and $(\frac{h_M A_M P_A}{G c_{pM}})$ with (L/G) for $Re = 8.766 \cdot 10^4$ with Flat Mat.

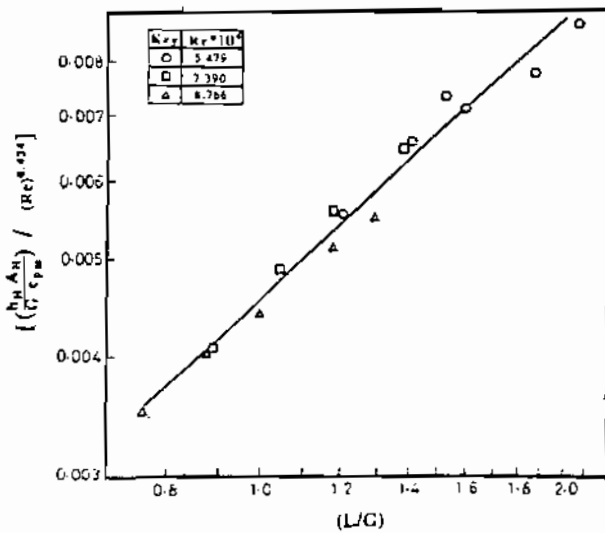


Fig.17 Correlation Between $[(\frac{h_M A_M}{G c_{pM}}) / (Re)^{0.434}]$ and (L/G).

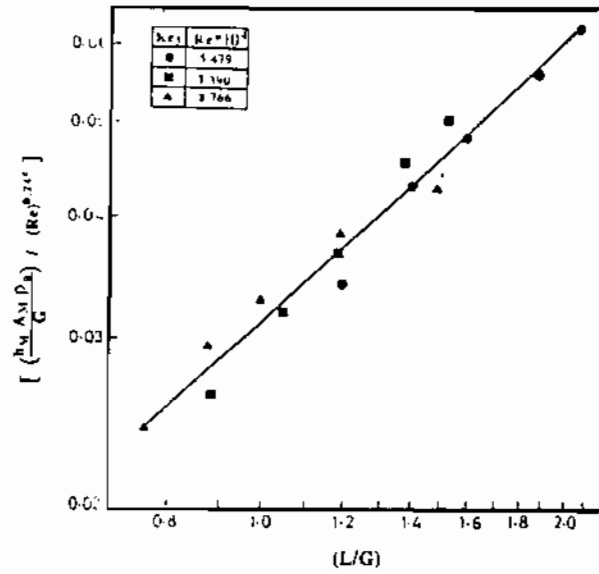


Fig. (8) Correlation Between $[\frac{h_m A_m \rho_a}{G}] / (Re)^{0.245}$ and (L/G) . with Flat Mat.

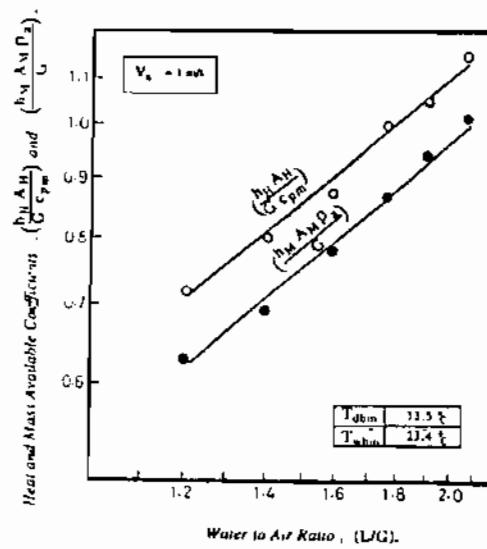


Fig. (9) Variation of $(\frac{h_m A_m}{G c_{p,m}})$ and $(\frac{h_m A_m \rho_a}{G})$ with (L/G) for $Re = 5.45 \times 10^4$, with Flat Mat.

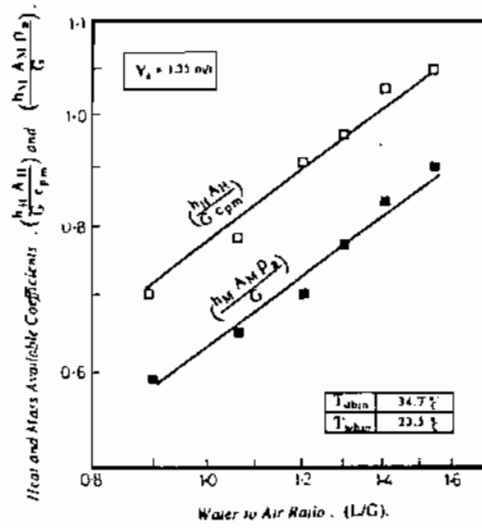


Fig. (10) Variation of $\left(\frac{h_{11} A_{11}}{G c_{p,m}}\right)$ and $\left(\frac{h_M A_M P_A}{G}\right)$ with (L/G) for $Re = 7.36 \times 10^4$. with Corrugated Mat.

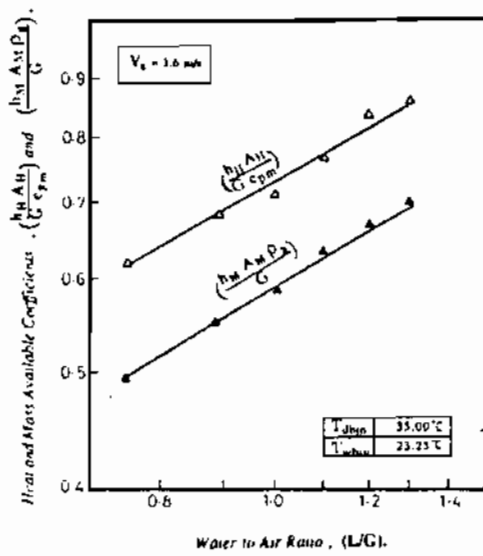


Fig. (11) Variation of $\left(\frac{h_{11} A_{11}}{G c_{p,m}}\right)$ and $\left(\frac{h_M A_M P_A}{G}\right)$ with (L/G) for $Re = 8.728 \times 10^4$. with Corrugated Mat.

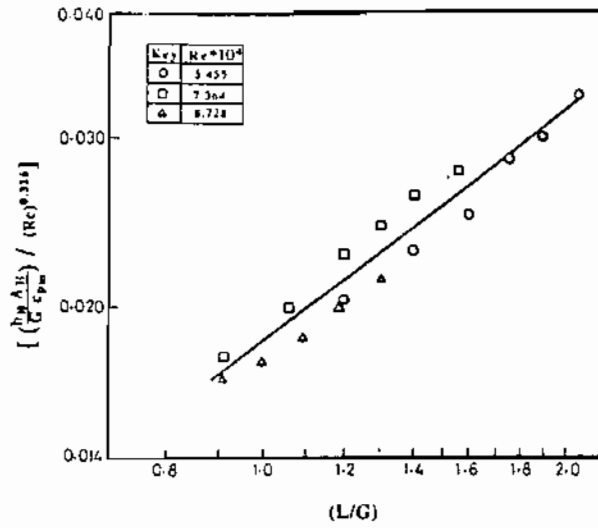


Fig.(12) Correlation Between $[(\frac{h_M A_M}{G c_{pM}}) / (Re)^{0.316}]$ and (L/G) .
With Corrugated Mat.

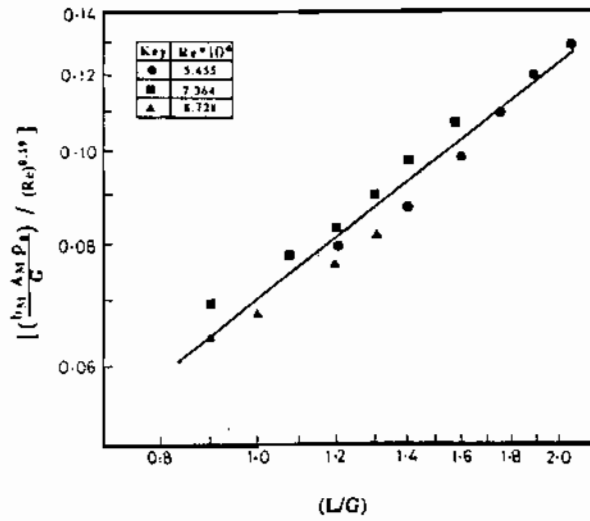


Fig.(13) Correlation Between $[(\frac{h_M A_M P_A}{G}) / (Re)^{0.19}]$ and (L/G) .
With Corrugated Mat.

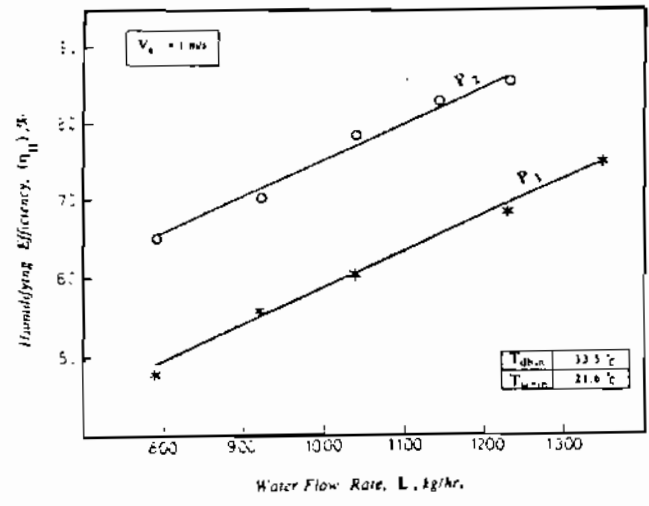


Fig (14) Variation of Humidifying Efficiency (η_{II}) with Water Flow Rate (L) For flat (P_1) and Corrugated (P_2) Mats.